

Fabry-Perrot Cavity-based Silicon Photonic Thermometers with Ultra-small Footprint and High Sensitivity

Nikolai N. Klimov^{1,2}, Thomas Purdy³, and Zeeshan Ahmed²

¹Joint Quantum Institute, University of Maryland, College Park, MD 20742

²Thermodynamic Metrology Group, Sensor Science Division, Physical Measurement Laboratory, National Institute of Standards and Technology, Gaithersburg, MD 20899

³Quantum Optics Group, Quantum Measurement Division, Physical Measurement Laboratory, National Institute of Standards and Technology, Gaithersburg, MD 20899

Abstract: In this work we report on the development of silicon photonic temperature sensors with ultra-small footprint and high temperature sensitivity as an alternative solution to legacy-based resistance thermometers.

1. Introduction

Resistance thermometry is a time-tested method for temperature measurements [1]. Due to their high sensitivity to environmental variables such as mechanical shock and humidity, resistance thermometers require frequent recalibrations. These fundamental limits of resistance-based approach have spurred substantial interest in the development of photonic-based temperature sensors as a viable alternative [2–4]. A wide variety of innovative photonic sensors have been proposed including macroscale functionalized dyes [5], hydrogels [6], fiber Bragg grating (FBG) sensors [2,3,5], and microscale silicon photonic devices [7–10]. In this study we explore temperature dependent responses of two Fabry-Perrot cavity-based silicon photonic devices, the silicon waveguide Bragg grating cavity (Si WBG-C) and the silicon photonic crystal nanobeam cavity (Si PhC-C). In the temperature range from 10° C to 40° C and when cladded with a PMMA^a, these devices have a sensitivity ($\delta\lambda/\delta T \approx 70$ pm/°C) that is at least 7x better than conventional FBG sensors [2,3,5].

2. Results and Discussion

The operating principle of silicon photonic temperature sensors is based on the high thermo-optic coefficient of silicon, which causes an almost linear shift of the resonance peak's wavelength with temperature. [11] Both types of silicon photonic thermometers, Si WBG-C and Si PhC-C, were fabricated at the NIST/CNST NanoFab facility using silicon-on-insulator (SOI) wafers applying conventional CMOS-technology via electron beam lithography followed by inductive plasma reactive ion etch (ICP RIE) of 220 nm-thick topmost silicon layer. After ICP RIE etch the devices were top-cladded with a 700 nm-thick PMMA protective layer.

The first type thermometer, a silicon waveguide Bragg grating cavity (Si WBG-C) is shown on FIG. 1a. It consists of silicon-on-insulator waveguide with width and thickness of 510 nm and 220 nm, respectively. The center part of the waveguide has a very small Fabry-Perrot cavity (327 nm long and 510 nm wide). The remaining part of the waveguide has periodic width modulation (60 nm in amplitude and a pitch of 330 nm) that forms Bragg grating mirrors on both sides of the cavity. Each Bragg mirror consists of 100 periods. The total length of the Si WBG-C is ≈ 66 μ m.

Figure 1b shows a transmission spectrum measured at 20° C of the Si WBG-C thermometer cladded with PMMA. The stop-band is from 1553.5 nm to 1567.0 nm. (The right stop-band edge at 20° C is beyond of the range of our tunable wavelength C-band laser and is not seen on FIG. 1b). At 1560.3 nm there is a Fabry-Perrot cavity resonance with peak width of FWHM ≈ 500 pm and quality factor of $Q \approx 3,100$. As the temperature is increased from 15° C to 40° C, the Si WBG-C shows a systematic linear upshift of its resonance wavelength of ≈ 70 pm/°C (FIG. 1c).

^a Disclaimer: Certain commercial fabrication facility, equipment, materials or computational software are identified in this paper in order to adequately specify device fabrication, the experimental procedure and data analysis. Such identification is not intended to imply endorsement by the National Institute of Standards and Technology, nor is it intended to imply that the facility, equipment, material or software identified are necessarily the best available.

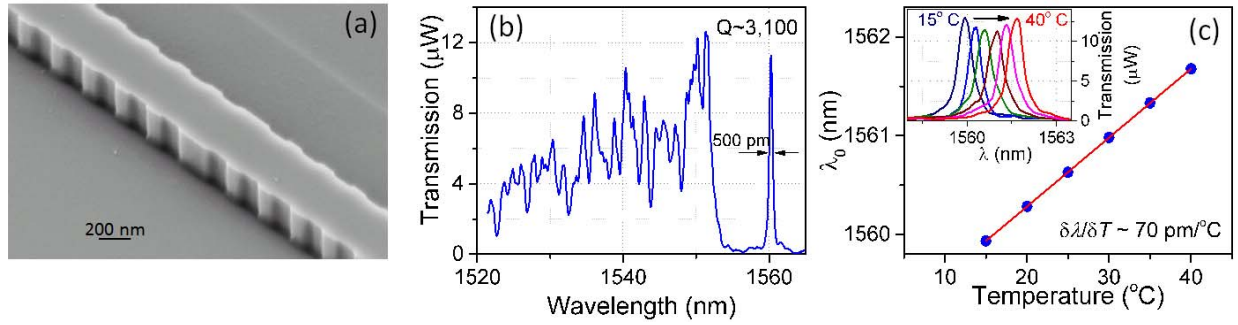


FIG.1 PMMA-cladded silicon Waveguide Bragg grating cavity thermometer. (a) SEM image of Si WBG-C before PMMA cladding. (b) Transmission spectrum of Si WBG-C thermometer measured at 20° C. (c) Temperature dependence of the resonance peak. Insert shows transmission spectrum of resonance peak measured at different temperatures: color curves counting from left to right correspond to $T = 15, 20, 25, 30, 35$ and 40° C, respectively.

The second type thermometer, the silicon photonic crystal nanobeam cavity, is shown in FIG. 2a. An 800 nm-wide silicon waveguide is patterned with a one dimensional array of subwavelength holes with diameters ranging from 170 nm to 230 nm that act as Bragg mirror. Our design follows the deterministic approach of Refs. [12,13], in which the Fabry-Perrot cavity is of zero length, while two adjacent photonic crystal Bragg mirrors feature a Gaussian field attenuation, thus maximizing the Q of the cavity. The light is coupled to the cavity by either end-fire coupling where input and output waveguides of width of 510 nm are adiabatically tapered to 800 nm and directly connected to the PhC-C (FIG. 2a), or by evanescently coupling from a bus waveguide placed within ≈ 200 -300 nm proximity from the PhC-C as shown on FIG. 3a.

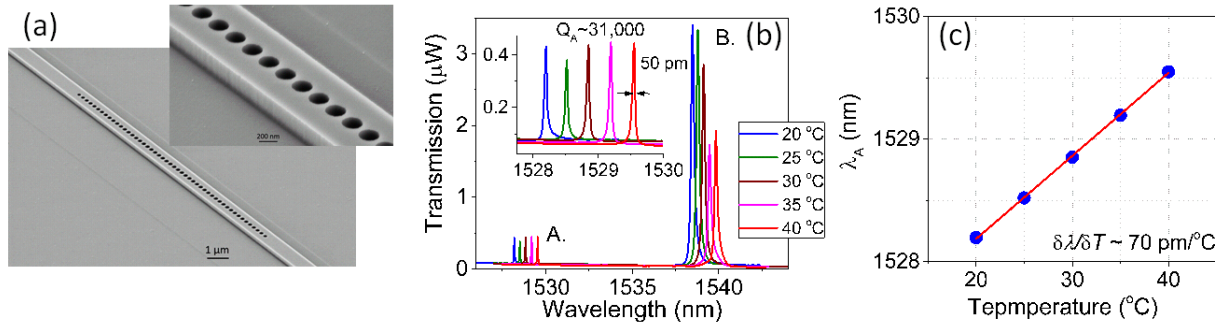


FIG.2 PMMA-cladded photonic crystal cavity (end-fire coupled) thermometer. (a) SEM image of PhC-C thermometer before PMMA cladding. (b) Transmission spectra of PhC-C thermometer taken at different temperatures. Fundamental and first mode are marked by A and B, respectively. Insert shows the transmission spectra of the resonance peak corresponding to the fundamental mode. (c) Temperature dependence of the resonance peak of the fundamental mode.

Figure 2b shows temperature dependence of transmission spectra of the fundamental mode A (≈ 1529 nm) and the first mode B (≈ 1540 nm) for Si PhC-C device with end-fire coupling. The FWHM for a fundamental mode resonance (insert to FIG. 2b) is ≈ 50 pm and $Q_A \approx 31,000$. Shown in FIG. 3b is the transmission spectrum measured at 20° of Si PhC-C evanescently coupled. For a wavelength range from 1520 nm to 1565 nm resonance peaks corresponding to the fundamental, 1st, 2nd, and 3rd are resolved. The quality factor of the fundamental mode (FWHM ≈ 60 pm, $Q_A \approx 26,000$) is very comparable to the PhC-C sensors shown on FIG. 2. Similar to Si WBG-C sensors, Si PhC-C thermometer, when cladded with PMMA, shows a linear upshift of resonance wavelength as temperature increases (FIGs. 2c and 3c) with sensitivity of ≈ 67 -70 pm/°C.

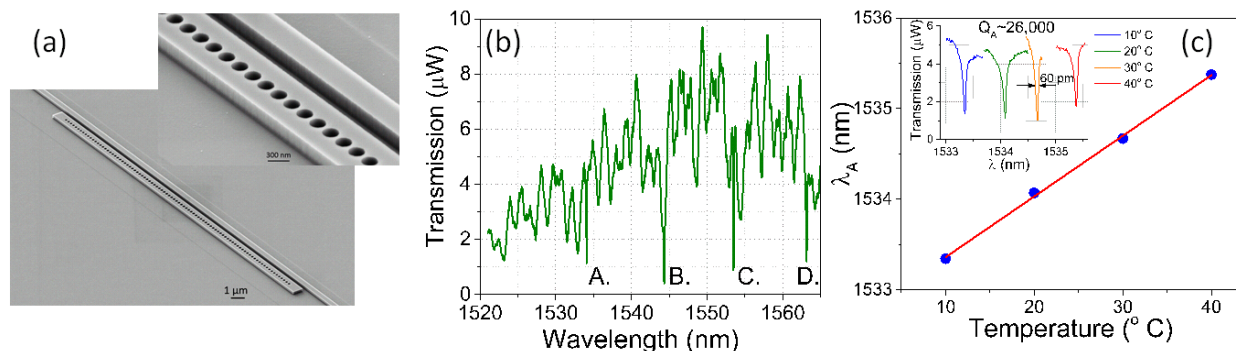


FIG.3 PMMA-cladded photonic crystal cavity (evanescently coupled) thermometer. (a) SEM image of PhC-C thermometer before PMMA cladding. (b) Transmission spectrum of PhC-C thermometer measured at 20° C. Fundamental, 1st, 2nd and 3rd mode are marked by A , B, C and D, respectively. (c) Temperature dependence of the resonance peak corresponding to the fundamental mode. Insert shows the transmission spectrum at different temperatures of the fundamental mode.

3. Summary

In this work we examine the temperature dependent response of our nanoscale Si WBG-C and Si PhC-C photonic sensors cladded with a PMMA protective layer over the temperature range from 10° C to 40° C and we demonstrate the temperature sensitivity ($\delta\lambda/\delta T \approx 70 \text{ pm}/^\circ\text{C}$) is at least 7x better compared to the sensitivity of conventional fiber Bragg grating (FBG) sensors. This sensitivity is comparable to the sensitivity of silicon ring resonator-based thermometers [7–10]. We expect that cladding silicon photonic sensors with silicon dioxide will further improve the device’s sensitivity. While WBG-C and PhC-C sensors have comparable temperature response, the later type has approximately a 10x narrower resonance peak as compared to WBG-C. We expect that the narrower linewidth of PhC-C thermometer will reduce combined measurement uncertainties by at least a factor of ten. In addition, the PhC-C has a smaller footprint. Both WBG-C and PhC-C sensors also allow for unambiguous determination of the fundamental mode. In summary, we have demonstrated that PhC-C and WBG-C sensors, fabricated using CMOS technology, are viable photonic temperature sensing solutions.

Acknowledgement

The authors acknowledge the NIST/CNST NanoFab facility for providing opportunity to fabricate silicon photonic temperature sensors.

References

- [1] G. F. Strouse, NIST Spec. Publ. **250**, 81 (2008).
- [2] S. J. Mihailov, Sensors **12**, 1898 (2012).
- [3] A. Kersey and T. A. Berkoff, IEEE Photonics Technol. Lett. **4**, 1183 (1992).
- [4] Y.-J. Rao, D. J. Webb, D. . Jackson, L. Zhang, and I. Bennion, J. Light. Technol. **15**, 779 (1997).
- [5] J. S. Donner, S. A. Thompson, M. P. Kreuzer, G. Baffou, and R. Quidant, Nano Lett. **12**, 2107 (2012).
- [6] E. M. Ahmed, J. Adv. Res. **6**, 105 (2015).
- [7] M.-S. Kwon and W. H. Steier, Opt. Express **16**, 9372 (2008).
- [8] B. Guha, K. Preston, and M. Lipson, Opt. Lett. **37**, 2253 (2012).
- [9] G.-D. Kim, H.-S. Lee, C.-H. Park, S.-S. Lee, B. T. Lim, H. K. Bae, and W.-G. Lee, Opt. Express **18**, 22215 (2010).
- [10] H. Xu, M. Hafezi, J. Fan, J. M. Taylor, G. F. Strouse, and Z. Ahmed, Opt. Express **22**, 3098 (2014).
- [11] G. Cocorullo, F. G. D. Corte, and I. Rendina, Appl. Phys. Lett. **74**, 3338 (1999).
- [12] Q. Quan, P. B. Deotare, and M. Loncar, Appl. Phys. Lett. **96**, 203102 (2010).
- [13] Q. Quan and M. Loncar, Opt. Express **19**, 18529 (2011).